Reference: *Biol. Bull.* **231:** 130–141. (October 2016)

Covering Ground: Movement Patterns and Random Walk Behavior in *Aquilonastra anomala* Sea Stars

AMANDA C. LOHMANN[1,*], DENNIS EVANGELISTA[2], LINDSAY D. WALDROP[3], CHRISTOPHER L. MAH[4], AND TYSON L. HEDRICK[1]

[1] *Department of Biology, University of North Carolina at Chapel Hill, Chapel Hill, North Carolina 27599;* [2] *Department of Weapons and Systems Engineering, United States Naval Academy, Annapolis, Maryland 21401;* [3] *Division of Natural Sciences, University of California, Merced, Merced, California 95343; and* [4] *Department of Invertebrate Zoology, National Museum of Natural History, Smithsonian Institution, Washington, D.C., 20013*

Abstract. The paths animals take while moving through their environments affect their likelihood of encountering food and other resources; thus, models of foraging behavior abound. To collect movement data appropriate for comparison with these models, we used time-lapse photography to track movements of a small, hardy, and easy-to-obtain organism, *Aquilonastra anomala* sea stars. We recorded the sea stars in a tank over many hours, with and without a food cue. With food present, they covered less distance, as predicted by theory; this strategy would allow them to remain near food. We then compared the paths of the sea stars to three common models of animal movement: Brownian motion, Lévy walks, and correlated random walks; we found that the sea stars' movements most closely resembled a correlated random walk. Additionally, we compared the search performance of models of Brownian motion, a Lévy walk, and a correlated random walk to that of a model based on the sea stars' movements. We found that the behavior of the modeled sea star walk was similar to that of the modeled correlated random walk and the Brownian motion model, but that the sea star walk was slightly more likely than the other walks to find targets at intermediate distances. While organisms are unlikely to follow an idealized random walk in all details, our data suggest that comparing the effectiveness of an organism's paths to those from theory can give insight into the organism's actual movement strategy. Finally, automated optical tracking of invertebrates proved feasible, and *A. anomala* was revealed to be a tractable, 2D-movement study system.

Received 3 December 2015; accepted 12 July 2016.

* To whom correspondence should be addressed. E-mail: alohmann@live.unc.edu.

Introduction

Many organisms forage, or move through the environment in search of food, but the ways they determine how to move (when to turn, how long to go in one direction, how to incorporate cues, how to change patterns given different food distributions) are still not well understood. The search path an organism takes affects its likelihood of encountering food or other resources, and different paths are more effective in different environments (Bartumeus *et al.,* 2005; Johnson *et al.,* 2008). Different random walk models have been proposed as ways to understand and simulate search behaviors. In such models, animal movements are modeled as discrete steps (vectors) between subsequent animal positions. For an animal moving in two dimensions (2D), the steps are typically characterized by two random variables representing 1) step length and 2) direction or turn angle. Three common random walk models are Brownian motion, Lévy walks, and correlated random walks (Bartumeus *et al.,* 2005).

Brownian motion has been used to model movement of animals, including feeding sharks (Humphries *et al.,* 2010) and insect pests (Petrovskii *et al.*, 2012). Brownian motion is predicted to occur when an animal is feeding in an area with high densities of food (Humphries *et al.*, 2010), and is likely to be the consequence of frequent encounters with resources (de Jager *et al.,* 2013). Because steps are often truncated by food encounters, step length is correlated with the spatial distribution of food items. Brownian motion is

observed when the steps are "short" and in uniformly random directions. Step lengths are typically drawn from an exponentially decaying distribution or a finite distribution, such as Gaussian, Rayleigh, or chi-squared; all result in similar overall behavior with generally short steps (Mörters and Peres, 2010). Turn angles (α) are drawn from a uniform distribution (Bartumeus *et al.*, 2005). The relatively short steps and lack of directionality result in a walker frequently returning to previously visited areas and experiencing slow movement away from the starting location (Viswanathan *et al*., 1999), which could keep it within areas of high-food density.

In contrast to Brownian motion, Lévy walks include rare, relatively "long" steps. Step lengths are typically drawn from a "fat-tailed" distribution such as a power-law (*e.g.,* Pareto) (Newman, 2005), where the exponent of the power law is $1<\mu\leq3$ (thus decreasing more slowly than exponential). Turn angles are drawn from a uniform distribution (Bartumeus *et al.*, 2005). Both step length and turn angle are uncorrelated and independent of one another. The occasional long steps are hypothesized to result in efficient searching when resources are located in sparsely and randomly distributed patches, in part because a Lévy walker is less likely to revisit a previously visited site than a walker without occasional long steps (Viswanathan *et al.*, 1999). Field studies have reported Lévy patterns in a number of animals, including honey bees (Reynolds *et al.*, 2007), spider monkeys (Ramos-Fernández *et al.*, 2004), human hunter-gatherers (Raichlen *et al.*, 2014), sharks, bony fishes, sea turtles, and penguins (Sims *et al.*, 2008). However, these results are controversial due to questions about the accuracy of tracking methods and statistical techniques (Benhamou, 2007; Petrovskii *et al.,* 2011; Edwards *et al.*, 2012; Jansen *et al.,* 2012; Pyke, 2015).

Both the Brownian and Lévy models discussed here are discretized idealizations of foraging paths, in which the discrete time intervals are longer than any turning or movement dynamics. This need not be the case, and correlated random walks can capture the short-term, directional nature of movement by using turn angles drawn from a nonuniform distribution such as a wrapped normal or von Mises with a peak at zero degrees (Bartumeus *et al.*, 2005). Typically, as in Brownian walks, correlated random walks have a finite or exponentially decaying step length distribution; only the distribution of turn angles is different (Kareiva and Shigesada, 1983; Crist *et al.,* 1992; Bartumeus *et al.*, 2005). Movements of animals, including beetles (Crist *et al.,* 1992), caribou (Bergman *et al.*, 2000), and ants (Sendova-Franks and Van Lent, 2002) have been modeled as correlated random walks at timescales short enough that directional persistence mattered.

Different movement patterns will be effective when food is in the nearby vicinity *versus* when it is not, so some organisms exhibit changes in movement behaviors triggered by food-related sensory cues. Two commonly observed changes are decreased velocity and increased turning rates, which, presumably, keep the organism near the food. For example, the ciliate *Favella* sp. and the protistan predator *Oxyrrihs marina* move more slowly in the presence of prey stimuli (Buskey and Stoecker 1989; Menden-Deuer and Grünbaum 2006). These organisms and the sea star *Astropecten articulatus* show increased turning rates in the presence of prey stimuli (Buskey and Stoecker 1989; Beddingfield and McClintock, 1993; Menden-Deuer and Grünbaum 2006).

Based on the large number of studies reporting Lévy walks in diverse taxa and the theoretical advantages of Lévy walks in environments such as the ocean floor, where food is patchily distributed, we hypothesized that we would observe Lévy walks in sea stars. We tested this hypothesis by comparing movements of *Aquilonastra anomala* (H. L. Clark, 1921) to random walk models. First, we obtained step lengths and turn angles by filming the animals in time lapse as they moved through the tank, tracking them using computer vision methods. We then used maximum likelihood estimation (MLE) to fit parameters under the different model assumptions. Finally, we ran simulations using the fitted parameters from MLE and determined the walks' likelihood of encountering targets at different distances from the starting position, as a measure of the relative search performance of the different random walk strategies.

We also hypothesized that when food is nearby, *A. anomala* would move more slowly and exhibit larger and more frequent turns in order to remain in the vicinity of the food. To test this theory, we used the same filming and tracking setup under two treatments: with and without a chunk of clam present in the tank. From the track data, we then compared speed, distance traveled, time spent moving, and turning rate between trials with clam *versus* without clam.

Materials and Methods

Collection, maintenance, and identification of animals

Eleven small sea stars (0.5–0.75 cm in diameter from arm tip to arm tip) were obtained from saltwater aquaria maintained for other research in the Department of Mathematics of the University of North Carolina at Chapel Hill (UNC). When not in trials, the sea stars were maintained at 22 °C and 32–34 psu in a tank containing other invertebrates (anemones, hermit crabs, and a sea urchin). The tank population was fed TetraMin Tropical Flakes (Tetra U.S., Blacksburg, VA) twice a week, and the sea stars also fed on algae growing on the glass.

Sea stars were identified based on recent revisionary work on the Asterinidae by O'Loughlin and Waters (2004) and O'Loughlin and Bribiesca-Contreras (2015), and by comparison with specimens from the National Museum of

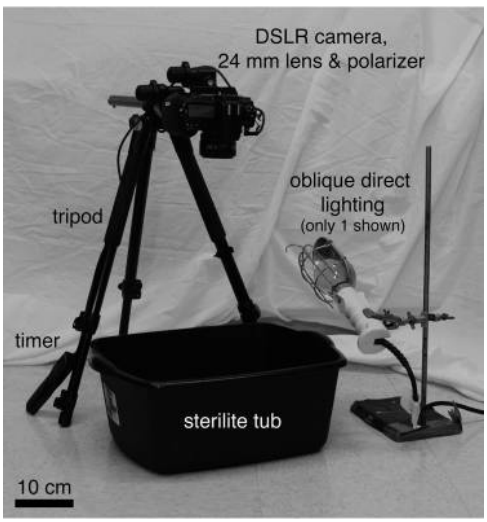

Figure 1. Filming arena and setup. Sterilite (Townsend, MA) tub dimensions (lwh) are 40 × 33 × 16 cm. DSLR, digital single-lens reflex.

Natural History (NMNH) in Washington, D.C. Based on the presence of superambulacrals, spine morphology, and the fissiparous nature of the specimen examined, the species was determined to be *Aquilonastra anomala* (Clark, 1921), whose documented range is in the central west Pacific Ocean. However, because these specimens were obtained *via* the aquarium trade and were observed in the context of Caribbean "live rock," it seems likely that they had undergone artificial transport away from their original setting. Possible tropical Atlantic species were compared and rejected based on collections of the NMNH collections and relevant literature (*e.g.*, Clark and Downey, 1992). Small fissiparous asterinids similar to this species are widely observed in the aquarium trade, but it is unclear if they are all the same species. This report represents one of the first published identifications of this species from transported aquarium conditions.

Experimental setup

Animals were filmed in an arena (Fig. 1) consisting of a 17-liter tub (Sterilite, Townsend, MA), dimensions (lwh) 40 × 33 × 16 cm, lined with black gravel, and filled with artificial seawater (ASW) (InstantOcean, Blacksburg, VA). Artificial seawater temperature remained near 24.1 °C for the duration of the 8 h of data collection. Salinity was maintained between 32 and 34 psu. To clean the tub between each trial (once a day), all sea stars were removed and the tub and gravel were rinsed twice with distilled water and once with ASW, before new ASW was added. During cleaning, sea stars were removed for 10 min, during which the lights in the room were turned off. The tub was placed on the floor in a small, windowless room with overhead fluorescent lights, and no one was present during the 8 h of data collection. Four days before the first trial, sea stars were placed in the filming tank in the room, with the overhead lights and the two 60-W lights used to illuminate the tank (see next section) turned on. During these 4 acclimation days, water changes were performed on the same schedule as during the trials and sea stars were not fed. During the 10 days of trials, sea stars were kept in the tub and not given food besides the clam pieces in the tub during the trials with clam. The trials were performed so that sea stars experienced 18 h of light during filming, followed by 6 h of darkness between trials.

All trials began by scattering the 11 sea stars across the tub; sea stars were placed on the substratum so that they were roughly evenly spaced. To test the effect of a food cue on sea star movements, a clam treatment, in which a chunk of canned clam (Fancy Whole Baby Clams; Bumble Bee Seafoods, San Diego, CA) approximately 0.5 cm in diameter, was used, and placed near the center of the tub. Sea stars are often scavengers, and to ascertain whether *Aquilonastra anomala* would feed on the clam, we placed a few chunks in their tank several weeks before we began the experiment. We observed that multiple sea stars did move onto the clam chunk and appear to feed. Ten total trials, five controls without clam and five with clam, were carried out in random order. Trials began between 22:00 and 22:30, and sea stars were filmed for a total of 18 h. Animals were not fed between trials.

The first 10 hours were considered an acclimation period, and only movements in the last 8 h were analyzed. Within the acclimation period, the first h was a period of extremely high activity, in which nearly all sea stars moved rapidly throughout the tank. Following this initial high activity, sea stars were mostly dormant until around the tenth hour, corresponding with 08:00 to 08:30, when activity increased, and remained at that level until the end of the trial. During the acclimation period, there was no difference in the behavior of the sea stars between trials with and without clam. During a test trial initiated at 16:00, sea stars also showed an uptick in activity about 10 h later (02:00), as well as no additional increase in activity at 08:00. Therefore, we chose to align trials based on time elapsed rather than wall clock time, since the sea stars were placed in the tank. All data reported here are from elapsed time 10:00 to 18:00.

Because of the possibility of temperature affecting overall activity, we verified that the lights used for filming did not appreciably raise the temperature of the seawater, and that temperature was constant during trials. An aquarium thermometer was placed in the tank and the temperature was recorded every half h for 15 h. Temperature started at 22.3 °C and increased by 1.8 °C per half-h, leveling off at 24.1 °C at elapsed time 10:00.

In trials with the clam treatment, all sea stars that actually encountered the clam chunk (zero sea stars (one trial), one

sea star (one trial), two sea stars (one trial), and three sea stars (two trials)) stopped moving and appeared to feed.

Time-lapse filming and automatic tracking

A Nikon digital single-lens reflex (DSLR) camera (D70s or D300s; Nikon, Tokyo, Japan) fitted with a 24-mm f/2.8 lens (NIKKOR; Nikon) was mounted on a tripod (Manfrotto, Cassola, Italy) to take images from directly above the tank (Fig. 1). An interval timer (Aputure, Shenzen, China) attached to the camera triggered the shutter every 8 s to provide time lapse. One 60-W, incandescent light was placed on either side of the tub at a height of 40 cm to provide illumination for photos. Black poster board was placed above the camera and against the wall behind the tub to eliminate reflections. The lens was also fitted with a linear polarizer (Tiffen, Hauppage, NY), rotated to eliminate further reflections from the free surface. Before the start of each trial, we obtained a 2D calibration using images of a ruler placed on the substratum.

We automatically detected and tracked sea stars in all videos, using specially written scripts in Python (Python Core Team, 2015) (Fig. 2). A sample video of tracked sea stars is available (see video online). Methods were similar to those used previously in automatic detection of ruby-throated hummingbirds (Sholtis *et al*., 2015) and cliff swallows (Shelton *et al.*, 2014). Here, a Haar cascade (Viola and Jones, 2001), implemented in the OpenCV library (Bradski, 2008), and trained using a manually digitized subset of 112 randomly selected images from the data set, was used to identify bounding box regions in which an *Aquilonastra anomala* was detected (Fig. 2b). We then applied Kalman filters to match the detections with tracks by creating state observers for each track and assigning new detections to preexisting tracks or spawning new tracks as needed. At the end of all automatic steps, a human quality assurance check (Fig. 2c) was used to separate out false detections, verify identities, and join tracks that had become divided during processing. Following tracking, we applied the linear calibration obtained above to convert from pixel coordinates to a 2D, real-world coordinate system. Source code for tracking steps and the quality assurance tool are available from Evangelista (2014). Downstream calculations were accomplished in both R (R Core Team, 2015) and Python (ver. 2.7; Python Core Team, 2015).

As a result of the Haar cascade search, the automatic tracking process can introduce small (1–2 pixels), uncorrelated errors in position that may affect the integration; we therefore smoothed the tracks by decimating the position data to every 25th frame and interpolating between these frames with a cubic spline, using the first derivative of the spline to estimate the components of velocity, v_x and v_y. The 25-frame interval corresponds to 200 s, during which moving sea stars traveled a mean of 3 cm; spline fits were also verified by plotting.

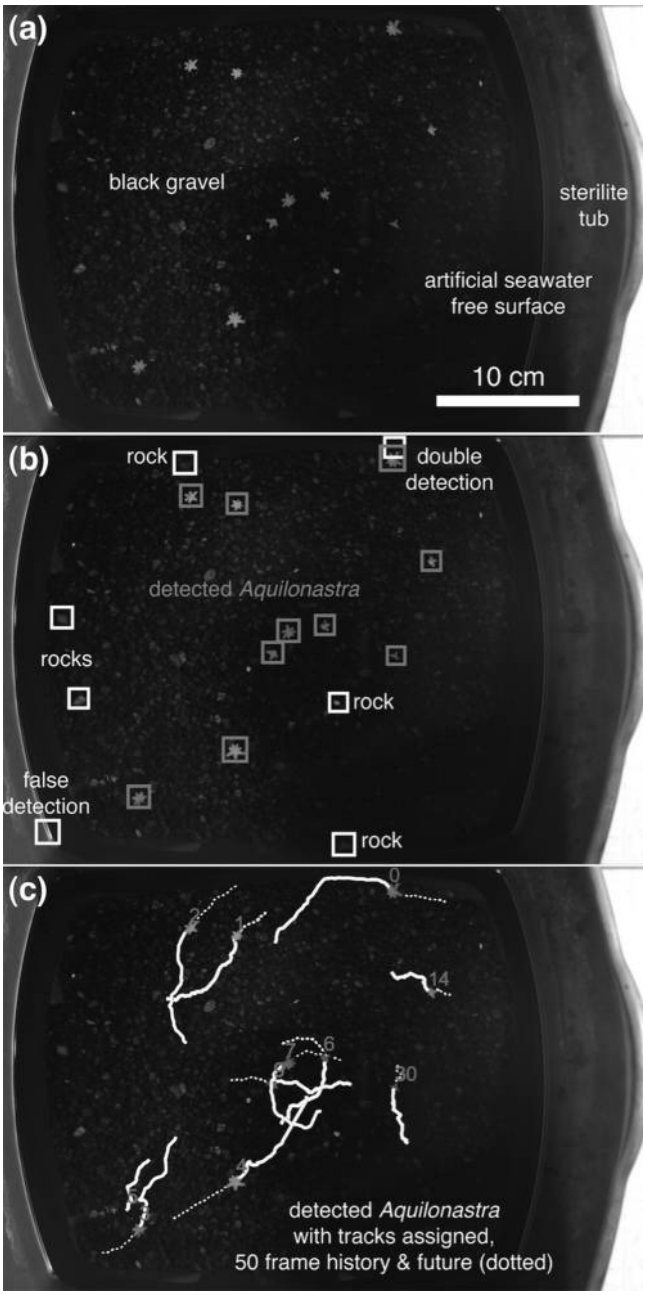

Figure 2. The tracking process of *Aquilonastra anomala*, showing (a) raw image, (b) initial detection, and (c) following automatic track assignment and manual quality assurance check.

When comparing the sea stars' movements to random walk models, we used the sea star's positions from every 25th frame. Sampling at too fine a scale is problematic; small wobbles in the animal's position that have nothing to do with the animal's overall forward motion can have undue influence on the analysis, as can measurement errors. For example, the detected sideways movement of a sea star

tilting slightly as it crawls over a slanted piece of gravel should not affect our results. Our autocorrelation analysis showed that at time intervals less than 25 frames, sea star movements are highly correlated time series and therefore do not provide useful information about the animals' overall movement. Thus, to avoid measuring minuscule changes in position that are too small to give information about the animal's path, or that are unrelated to the animal's overall motion, we used 25 frames (200 s) as the time interval for analysis.

Maximum likelihood estimation (MLE) of movement parameters

We examined four movement parameters: time-based step length, straight-line step length, heading (θ), and turn angle (α). Time-based step length is the distance between a sea star's positions at sequential time steps; straight-line step length is the distance traveled between turning events; heading is the direction of its movement relative to axes imposed on the tank; and turn angle is the difference in angle between sequential headings. Straight-line step length analyses are discussed further (see next section). Both time-based steps and straight-line steps that occurred when a sea star traveled along the edge of the arena were removed from the analysis.

In maximum likelihood estimation (MLE) of movement parameters we used the same sea star movement data from 10:00 to 18:00. For MLE, the raw data were not smoothed, and the effect of varying time scales (25 and 200 frames) was considered in computing step lengths and angles. Because step length and angle distributions for individuals appeared similar, and because running the analysis separately on clam and no-clam trials had virtually no impact on the fit parameters, the MLE analyses presented here pooled all data.

Brownian and Lévy models assume that each step (length and direction) is independent of the previous step; therefore, we first examined the autocorrelation after Denny *et al.* (2009) of time-based step length, heading (θ), and turn angle (α) considering no decimation, as well as 25, 100, and 200 frames. To check the autocorrelation, each sequence was first normalized to obtain zero-mean unit variance: $y=(x-\bar{x})/s$, where $\bar{x}$ is the mean and s is the standard deviation. The discrete autocorrelation $R:-1<R<1$, was then computed as the sliding sum, $R_{yy}[l]=\sum_n y[n]y[n-l]$, where R_{yy} denotes the correlation of y with itself, n is the frame number, and l is a frame lag at which the autocorrelation is to be computed. R provides a measure of how correlated a sea star's movements are with themselves at frame lag l. An additional measure is the decorrelation lag time, the time lag where R first crosses zero (Denny *et al.*, 2009). Autocorrelation was calculated using Python scripts and the SciPy (Jones *et al.*, 2015) and NumPy (van der Walt *et al.*, 2011) libraries.

Random walk models were then fitted using MLE. For each statistical model, the negative log-likelihood was computed under assumed parameters. The parameters were varied, using a limited-memory bounded Broyden-Fletcher-Goldfarb-Shanno (L-BFGS-B) optimization algorithm to find minimized negative log-likelihood. For MLE, we used Python and the SciPy and NumPy libraries. Steps and angles were estimated separately.

For turn angles, we considered two models: uniformly distributed and a circular normal (von Mises) distribution.

For time-based step lengths, we considered several models: uniform distribution (an uninformative null model); Lévy as a Pareto distribution; and Brownian and correlated random as exponential, Rayleigh, and chi-squared distributions. After MLE, models were compared using their respective Akaike Information Criteria (AIC), given by $AIC = 2k - 2ln(L)$, where L is the maximum value of the likelihood function for the model and k is the number of independently adjusted parameters within the model (Akaike, 1974; Burnham and Anderson, 2002; Evangelista *et al.,* 2014).

Analysis using straight-line step lengths

While Lévy walks can be defined using time-based step lengths (Ghaemi *et al.*, 2009; Majumdar**,** 2010), many biological analyses have examined Lévy walks using straight-line step lengths (for example, Reynolds *et al.,* 2007; Humphries *et al.,* 2012). We calculated straight-line step lengths by choosing a minimum turn angle and then looking at each time-based step; if the difference between the initial heading of the current straight-line step and the heading of the next time-based step was less than the minimum turn angle, the time-based step was absorbed into the straight-line step; if the difference in heading was greater than the minimum turn angle, the time-based step was considered the start of the next straight-line step (Reynolds *et al.*, 2007). Because AIC comparisons cannot be done between data sets, we did not compare fits to the straight-line step length distribution with fits to the time-based step length distribution. Instead, we used techniques described by Clauset *et al.* (2009) to determine whether a Pareto (that is, power law) distribution fit the straight-line step length distribution; we also tested an exponential fit for comparison. To check whether the specific minimum turn angle used had an impact on the results, we performed this analysis using straight-line steps generated with minimum turn angles ranging from 5° to 90° by 5°-increments (Reynolds *et al.,* 2007).

Simulation of random walks

To examine behavior in an unconstrained case of an infinitely large tank and to test the effect of different angle and step distributions, we simulated random walks based on the same models used to fit observed *Aquilonastra anomala* movements. A Python script was used to simulate random walks, using the same parameters obtained from MLE. In addition, the observed movement data were shuffled and resampled, with replacement, to provide an additional random walk case based on actual *A. anomala* movements. Step sizes and turn angles were obtained as random variables drawn from each distribution of interest, and these were then summed to obtain a walker's position at each 25th frame. The frames in between were then linearly interpolated.

Detectors 5 cm in diameter were modeled at radial distances from 5 cm to 1 m, to count when random walkers crossed through them. The number of hits and the number of walkers recorded at each detector were then tabulated to obtain the probability that a walker would hit the detector at least once during 8 h of simulated time. The simulation was initially conducted with 10,000 or 30,000 walkers; a convergence check was conducted with 1 million walkers to validate results. All results plotted here used the final result from 1 million walkers.

Movement with and without food

To examine the effect of the food cue on overall movement, we integrated the tracks to determine the total distance traveled, time spent moving, and average speed while moving. Total distance traveled was calculated as the sum $\Sigma V \cdot \delta t$, where speed $V = \sqrt{v_x^2 + v_y^2}$. Starfish were separately marked as "moving" if they moved more than a 2-pixel autodetection threshold. Time spent moving was then the sum of the time steps marked as moving. Similarly, the average speed while moving was the mean of V for time steps marked as moving. Calculations used Python; results were plotted and evaluated further in R.

To be able to compare differences in behavior of individual sea stars with and without clam, sea stars were identified across trials using size, shape, and number of arms. We then used a linear mixed-effects model to check for the effects of presence or absence of clam, trial, and individual on measures of overall movement.

Results

Autocorrelation

The autocorrelation for both step size and angle is shown in Figure 3. Autocorrelation is non-zero in both step length and heading out to a few hundred frames. Figure 4 compares the decorrelation time lag for step and heading, without and with clam. Step lag times are significantly different (*t*-test, $P = 0.01818$, $t = 2.1883$, $df = 30.795$) between no clam and clam, while heading lag times are not (*t*-test, $P = 0.1688$, $t = 0.969$, $df = 46.344$) (Fig. 4). Autocorrelation did not show individual effects when tested with a two-way ANOVA, either for individual effects ($P = 0.590$, $F = 0.8868$, $df = 16$) or for interactions between individual and treatment ($P = 0.472$, $F = 1.0017$, $df = 11$).

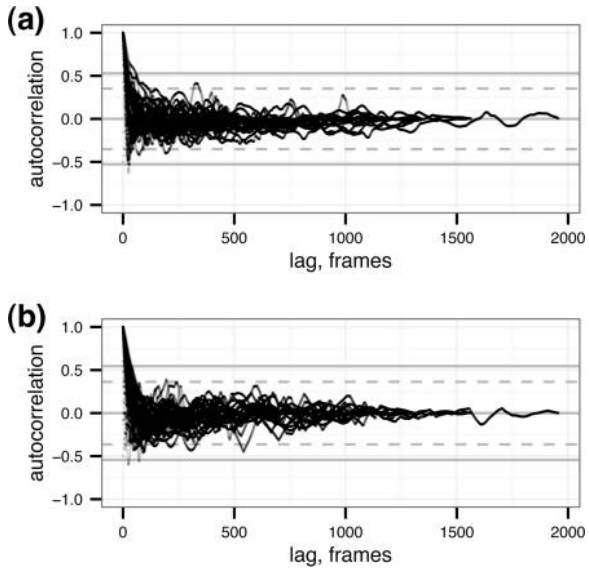

Figure 3. Autocorrelation for each starfish in (a) step size and (b) angle, showing that sea star movements are strongly correlated on this time scale (time between frames is 8 s). Confidence intervals of 95% and 99% are shown as solid and dashed gray lines, respectively. Sea star movements became uncorrelated at around 1600 s (200 frames).

Angle distribution and step distribution

The headings (θ) used by sea stars (Fig. 5) are approximately uniformly distributed, but with peaks at cardinal headings 0°, 90°, 180°, and −90°. The peaks are likely an experimental artifact resulting from the finite limits of the tank; otherwise, sea stars showed no preference for travel in a particular direction.

Distribution of frame-to-frame turn angles (α) showed a clear tendency towards smaller angles, meaning, sea stars tended to continue roughly straight (Fig. 6a, c); that is, their direction was correlated in time at time steps of 25 frames (200 s); at time steps of 200 frames (1600 s) the turn angles looked uniform and uncorrelated (Fig. 6b, d). Table 1A gives the results for MLE of turn angle distribution at time steps of 25 frames. The turns showed no bias towards either the left or right.

Time-based lengths of the sea stars are shown in Figure 7. Table 1B gives the results for MLE of step length.

For the Lévy analysis of straight-line step lengths, the Pareto fit was rejected by the Kolmogorov Smirnov statistic

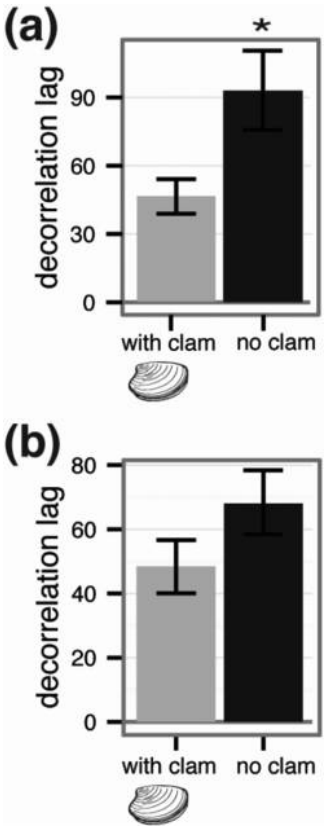

Figure 4. Decorrelation lag time for each starfish in (a) step size and (b) angle, for a step duration of 200 s (25 frames). Step lag times are significantly different (*t*-test, $P = 0.01818$, $t = 2.1883$, $df = 30.795$) between the no clam and clam trials, while angle lag times are not (*t*-test, $P = 0.1688$, $t = 0.969$, $df = 46.344$).

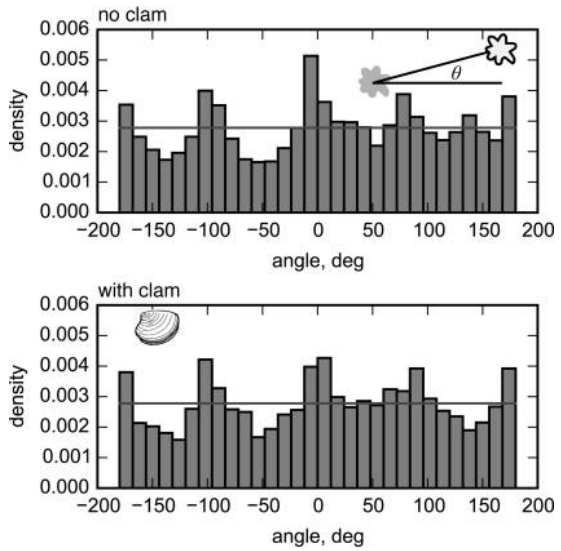

Figure 5. Heading (θ) distribution for (a) the no clam *versus* (b) clam trial, showing the direction of sea star movement in every step relative to the coordinate axis imposed on the tub; diagram in upper right of (A) indicates θ as the angle between the sea star's movement vector (previous position in gray and current position outlined) and the tank axis. The peaks at −180°, −90°, 0°, 90°, and 180° are likely artifacts of the tub, created by sea stars walking along the edges.

(D) for distributions generated with all tested minimum turn angles. The closest fit occurred when the minimum turn angle was 25° ($P = 10^{-5}$, where $P < 0.05$ rejects the fit, $D = 0.0878$), and the worst fit occurred with minimum turn angle of 5° ($P = 10^{-13}$, $D = 0.1200$) (Fig. 8). At a minimum turn angle of 25°, an exponential fit was slightly better ($P = 0.024$, $D = 0.0580$).

Simulation of random walks

Example random walks are shown in Figure 9. The resulting probability of detecting a 5-cm target at different target distances after an equivalent 8-h run is shown in Figure 10. Of the modeled walks, the Brownian walks had the highest success when the targets were short distances away (<7 cm); the modeled *Aquilonastra anomala* walk was the most successful for targets between about 7 cm and 22.5 cm; the correlated random walk was most successful for targets between 22.5 cm and 49 cm; and the Lévy walk was the most successful for targets farther away than 49 cm. For targets at all distances, the success curve of the modeled *A. anomala* walk was similar to that of the Brownian and correlated random walks, while the Lévy walk success curve showed distinct behavior (Fig. 10).

Movement with and without food

We created a linear mixed-effects model incorporating presence of clam as a fixed variable, and trial and individual as random variables. An ANOVA of the model found that the presence of clam had a significant effect on total distance traveled ($P = 0.0237$, $F = 5.5803$). Sea stars in trials without clam traveled 0.79 ± 0.11 m (mean ± SE), compared to 0.45 ± 0.10 m in trials with clam (Fig. 11a).

The difference in total distance traveled was due to a difference in time spent moving, not in speed when moving (Fig. 11b). There was no difference between the two groups in mean speed of the sea stars when moving (13.2 ± 0.6 m h^{-1} for no-clam trials and 12 ± 1 m h^{-1} for clam trials). However, among active sea stars, those in the no-clam trials spent more time moving (1.9 ± 0.17 h) than sea stars in the clam trials (1.2 ± 0.2 h); an ANOVA of a linear mixed-effects model found that $P = 0.0385$ ($F = 4.6138$).

No differences in turn angles between consecutive walk segments or in net to gross displacement ratios (both measures of how straight the sea stars' paths were) were found between the clam and no-clam trials.

Discussion

We compared the movements of *Aquilonastra anomala* sea stars to three random walk models (Brownian motion,

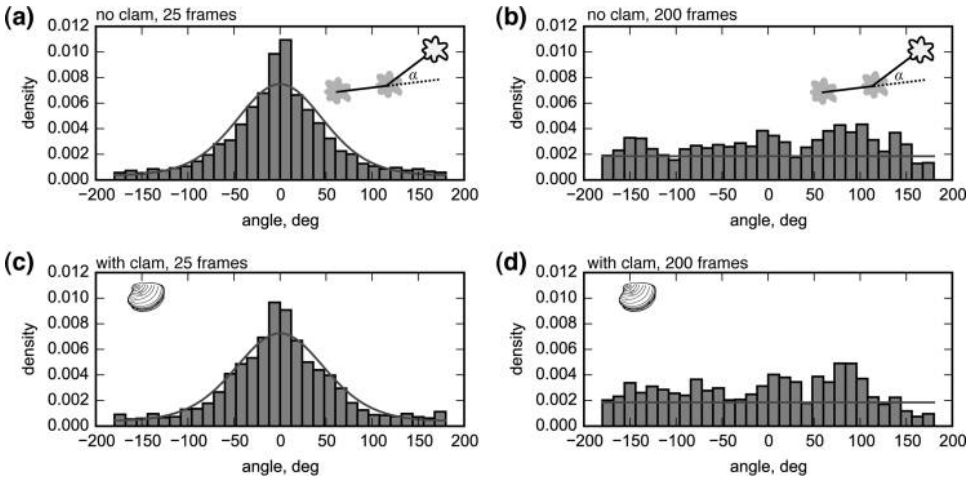

Figure 6. When sampled at short intervals (25 frames, left) (a) and (c), such that movements are still correlated, observed frame-to-frame angle changes (α) appear forward-skewed, indicative of a directionally correlated process, and are best approximated by a circular normal (von Mises) distribution. Sampling at longer intervals removes the forward skew (200 frames, right) (b) and (d), resulting in angles that are approximately uniformly distributed and would indicate a directionally uncorrelated process (see ΔAIC, Table 1A).

Table 1

MLE and AIC results of fitting random models to the turn angle and step length distributions of the sea star data

A. Turn angle (α)

Model	Parameters	Log likelihood	AIC	ΔAIC
Uniform	NA	−192308	384616	47,725
von Mises	$\mu = 0$ (fixed), $\kappa = 1.44587$	−168443	336891 (minimum)	0

B. Step length

Model	Parameters	Log likelihood	AIC	ΔAIC
Uniform	NA	37339	−74679	90,978
Pareto	$\alpha = 0.2212$	28808	−57615	108,042
Exponential	$\lambda = 26.3149$	72358	−144714	20,943
Rayleigh	$1/\kappa = 31.148958$	78573	−157144	8,513
Chi-squared	$df = 7.3437$, $1/\kappa = 193.2502$	82830	−165657 (minimum)	0

The best-fit model to turn angle distribution is the von Mises (circular normal), showing that direction is correlated at the scales examined and is consistent with a correlated random walk. The best-fit model for step length distribution is the chi-squared distribution, which is consistent with Brownian motion or a correlated random walk. In the von Mises (circular normal) distribution, μ is a measure of location and is analogous to the mean in a normal distribution, κ is a measure of concentration, and $1/\kappa$ is analogous to the variance of a normal distribution. In the Pareto distribution, α is the power parameter, and λ is the exponent parameter of the exponential distribution. In the Rayleigh distribution, $1/\kappa$ is the scale parameter. In the chi-squared distribution, *df* indicates degrees of freedom, and κ is the noncentrality parameter.

AIC, Akaike Information Criteria; MLE, maximum likelihood estimation; NA not applicable.

Lévy walks, and correlated random walks) by examining the sea stars' step length and turn angle distributions. At time steps of 200 s (25 frames), the distribution of time-based step lengths of *A. anomala* was well approximated by a chi-squared distribution (Fig. 7, Table 1B), and the distribution of turn angles was well approximated by a circular normal (von Mises) distribution (Fig. 6, Table 1A). Additionally, the distribution of straight-line step lengths was not well approximated by a Pareto distribution (and an exponential distribution used for comparison proved to be a slightly better fit) (Fig. 8). Therefore, our hypothesis that *A. anomala* would exhibit Lévy walks was not supported. Movements of *A. anomala* are instead well modeled as a correlated random walk.

We also looked at whether the presence of food cues in the tank would affect distance traveled, speed, and turning frequency. The sea stars spent less time moving in trials with food cues and, as we predicted, covered less distance; however, they did not exhibit slower speed when moving, nor did they turn more frequently.

Movements of Aquilonastra anomala *resembled a correlated random walk*

For *A. anomala*, step lengths appeared to have a finite distribution well approximated by a chi-squared distribution (Fig. 7, Table 1B), while turn angles at time steps of 200 s were not uniform, instead appearing circular normal (von Mises) (Fig. 6, Table 1A). We also observed significant autocorrelation in movements of up to fairly long duration (1600 s) (Fig. 3). We conclude that actual *A. anomala* movements most closely resemble a correlated random walk. Autocorrelation and non-uniform turn angles rule out

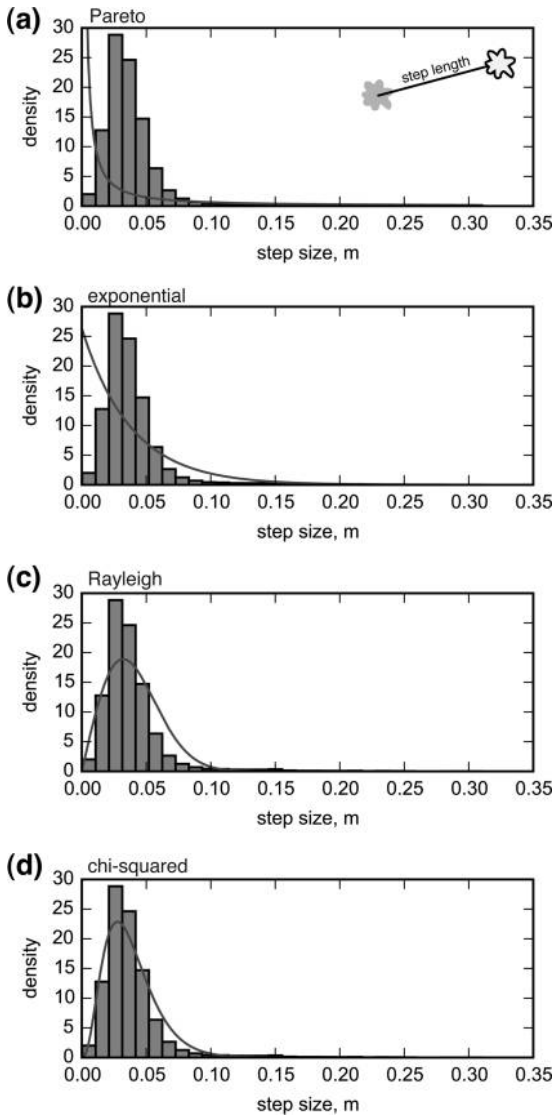

Figure 7. Time-based length distribution and fit to (a) Pareto, (b) exponential, and (c) Rayleigh and (d) chi-squared distribution. Pareto and exponential are not better models than a null hypothesis of uniform; chi-squared and Rayleigh do much better (see ΔAIC, Table 1B).

a Brownian model for time steps below 1600 s because Brownian motion assumes uncorrelated turn angles. The finite, small step sizes are not well modeled under Lévy assumptions. Furthermore, the searching performance of the modeled *A. anomala* walker was very similar to that of the modeled correlated random walker, further supporting the similarity of the two walks (Fig. 10).

If the movements were downsampled so that the interval between movements was more than 1600 s (about half an hour), the steps and angles would match an idealized Brownian walk but would still be dissimilar to a Lévy walk (Fig. 6b, d). However, such coarse time sampling may not always be desired in studies of animal motion. For example, examination of the trails of the asteroid *Oreaster reticulatus*

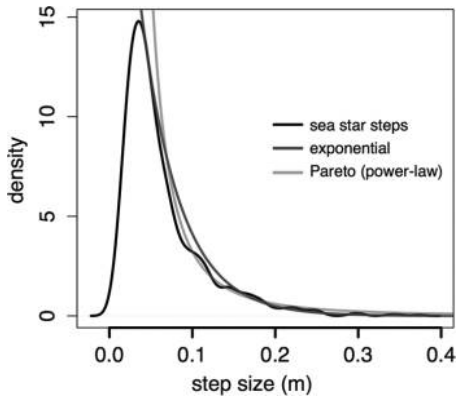

Figure 8. Straight-line step length distribution using a 25°-turn angle cutoff, and fit to Pareto and exponential distributions. Both fits were rejected by the Kolmogorov Smirnov statistic. For Pareto, the test found that $P = 0.00001$ ($D = 0.0878$), where $P < 0.05$ rejects the fit, while the exponential fit was slightly better ($P = 0.024$, $D = 0.0580$).

in the field have shown that these sea stars tend to travel between one and two body lengths between feeding events, and turn angles showed correlation at the study's time step size of 4 h, during which, at the animals' average speed, an individual would have traveled roughly 80 body lengths (Scheibling, 1981). In situations like this, where an animal's resource encounters take place at a scale much smaller than the scale at which angle autocorrelation disappears, modeling movement during foraging using non-directional models would miss relevant behavior.

Intermediate search behaviors outside of typical Brownian or Lévy assumptions may be more effective at middling distances and in ecologically relevant, bounded spaces.

Our simulations showed that the *Aquilonastra anomala* model had the highest encounter probability of the four

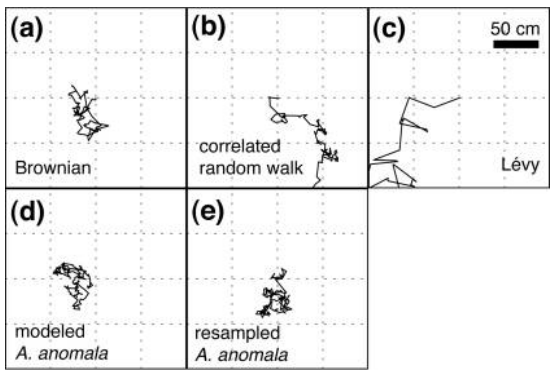

Figure 9. Example random walk simulations: (a) Brownian walk (exponential step length plus uniform angle); (b) correlated random walk (exponential step length plus von Mises angle); (c) Lévy walk (Pareto step length plus uniform angle), (d) modeled after observed behavior of *Aquilonastra anomala* (chi-squared plus von Mises), and (e) drawn from actual movements of *Aquilonastra anomala*.

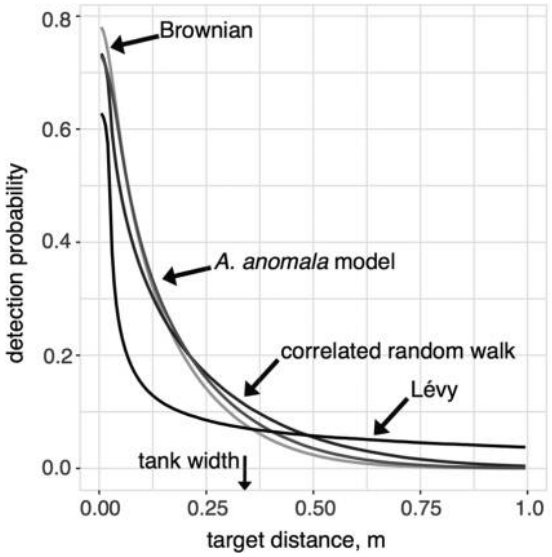

Figure 10. Probability of a random walker detecting a 5-cm target after 8 h. Results are shown for 1,000,000 random walkers. Brownian walk (light gray line) performs best at very short distances and the Lévy walk (black line), at long distances. For middling distances from 7 cm to 22.5 cm, the modeled *Aquilonastra anomala* performs best until the correlated random walker (mid-gray line) overtakes it. Tank dimensions, 40 × 33 cm.

models for targets between 7 cm and 22.5 cm from the starting point (Fig. 10). The Brownian model performed best at the shortest distances (< 7 cm); the correlated random walk model overtook the Brownian model at 16.5 cm, and overtook the sea star model at 22.5 cm. The curves of the Brownian, correlated random walk, and sea star models all showed similar behavior, while the Lévy walk model's curve looked very different. The Lévy walk became most effective at hitting targets at 49 cm from the start point, outperforming the other models when the target was at far distances, but doing comparatively poorly for distances below about 30 cm. The modeled sea star outperformed the Brownian, correlated random, and Lévy models at intermediate distances, and its success did not fall off as quickly at longer distances as that of the Brownian model. However, both the Brownian model and the sea star model were outperformed at longer distances by the correlated random walk model and the Lévy model.

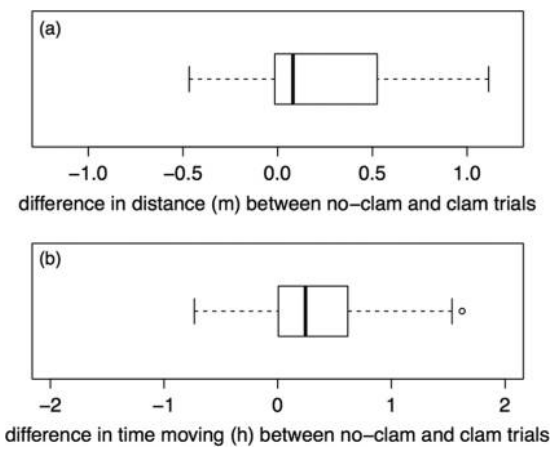

Figure 11. Difference between mean distance traveled (a) and mean time spent moving (b) in trials without clam *versus* trials with clam for each sea star. Sea stars in trials without clam traveled a mean distance of 0.79 ± 0.11 m (mean ± SE), compared with 0.45 ± 0.10 m in trials with clam (ANOVA on linear mixed-effects model, $P = 0.0237$, $F = 5.5803$). Sea stars in no-clam trials spent more time moving (1.9 ± 0.17 h, mean ± SE) than sea stars in the clam trials (1.2 ± 0.2 h) (ANOVA on linear mixed-effects model, $P = 0.0385$, $F = 4.6138$).

The sea stars in this study were in a small area (about 70 body lengths × 80 body lengths). This constraint is not necessarily biologically unrealistic, though, as many sea stars spend time in closed areas such as a tide pool or on the surface of a rock. Because Lévy walks have long step lengths and spread out quickly from the starting point, they are ineffective over a small area, and may not confer advantage in bounded environments. Large pelagic animals needing to search huge, essentially unbounded areas might benefit from a movement pattern resembling a Lévy walk. However, organisms that remain in a bounded environment, like on a rock or in the shelter of a coral clump or other structure, would benefit from a movement pattern (like Brownian motion or a correlated random walk) that thoroughly traverses a small region.

This study and others of random walk behavior operate under the assumption that recorded movements reflect animals that are searching for food (or another resource). Because the sea stars showed a tendency to bury themselves in the gravel and sit still for long periods of time, we find it likely that those that were moving were indeed searching for something. Furthermore, the fact that sea stars in tanks without clam covered more distance than sea stars in trials with clam suggests that they were searching for food cues.

Aquilonastra anomala *alter movements in the presence of food*

The decreased movement by sea stars when clam was present in the tank (Fig. 11a) is consistent with our hypothesis that *A. anomala* would move less in the presence of food to remain near the food. Rather than reduce their speed when moving, the sea stars spent less time moving (Fig. 11b) in the clam trials. We found no evidence to support our hypothesis that sea stars in the clam trials would turn more frequently or display paths with more curvature than sea stars in the no-clam trials.

Method considerations for future studies of movement behavior

The automatic tracking techniques presented here were able to accurately track sea stars in a large number of frames

in a shorter time than would have been possible with manual tracking. While our methods were employed in the lab, automatic optical tracking is potentially useful for field studies of sea stars or other marine invertebrates. Attempts to microchip sea stars revealed that the animals could transport tags within the coelom and clear them from their bodies (Olsen *et al.*, 2015), and a camera-based optical system that was stationary, in a fixed observatory or mounted on an autonomous vehicle could work well for field studies of species that tend to stay in a relatively small area.

Additionally, when choosing a time step for a movement study, our results reinforce the need to check the autocorrelation. If the goal is to examine long-time scale movement behavior using random walk models with uncorrelated steps, it is not necessary to sample at time scales at which movement is correlated. On the other hand, studies interested in taking into account smaller-scale movements and correlation should use time steps small enough to show autocorrelation, as coarser steps can mask details that may be relevant to the question at hand.

Acknowledgments

We thank L. Miller, the Miller Lab, and the Integrative Mathematical Physiology group at UNC for their advice and support of this project, and Jonathan Rader for assistance with the statistical analysis. This work was supported by the Office of Naval Research (grant no. N0001410109452 to TH and 8 others) and by the National Science Foundation (no. IOS 1253276 to TH).

Literature Cited

Akaike, H. 1974. A new look at the statistical model identification. *IEEE Trans. Automatic Control* **19:** 716–723.

Bartumeus, F., M. G. E. da Luz, G. M. Viswanathan, and J. Catalan. 2005. Animal search strategies: a quantitative random-walk analysis. *Ecology* **86:** 3078–3087.

Beddingfield, S. D., and J. B. McClintock. 1993. Feeding behavior of the sea star *Astropecten articulatus* (Echinodermata: Asteroidea): an evaluation of energy-efficient foraging in a soft-bottom predator. *Mar. Biol.* **115:** 669–676.

Benhamou, S. 2007. How many animals really do the Lévy walk? *Ecology* **88:** 1962–1969.

Bergman, C. M., J. A. Schaefer, and S. N. Luttich. 2000. Caribou movement as a correlated random walk. *Oecologia* **123:** 364–374.

Bradski, G. 2008. The OpenCV Library [Online]. Dr. Dobb's Journal of Software Tools. Available: http://www.drdobbs.com/open-source/the-opencv-library/184404319 [2015, Nov. 5].

Burnham, K. P., and D. R. Anderson. 2002. *Model Selection and Multimodal Inference: A Practical Information-Theoretic Approach*, 2nd ed. Springer-Verlag, New York.

Buskey, E. J., and D. K. Stoecker. 1989. Behavioral responses of the marine tintinnid *Favella* sp. to phytoplankton: influence of chemical, mechanical and photic stimuli. *J. Exp. Mar. Biol. Ecol.* **132:** 1–16.

Clark, A. M., and M. E. Downey. 1992. *Starfishes of the Atlantic*. Chapman & Hall, London.

Clark, H. L. 1921. *The Echinoderm Fauna of Torres Strait: Its Composition and Its Origin*. Carnegie Institution of Washington, Washington, D.C.

Clauset, A., C. R. Shalizi, and M. E. J. Newman. 2009. Power-law distributions in empirical data. *SIAM Rev.* **51:** 661–703.

Crist, T. O., D. S. Guertin, J. A. Wiens, and B. T. Milne. 1992. Animal movement in heterogeneous landscapes: an experiment with Eleodes beetles in Shortgrass Prairie. *Funct. Ecol.* **6:** 536–544.

de Jager, M., F. Bartumeus, A. Kölzsch, F. J. Weissing, G. M. Hengeveld, B. A. Nolet, P. M. J. Herman, and J. van de Koppel. 2013. How superdiffusion gets arrested: ecological encounters explain shift from Lévy to Brownian movement. *Proc. R. Soc. B Biol. Sci.* **281:** 20132605.

Denny, M. W., L. J. H. Hunt, L. P. Miller, and C. D. G. Harley. 2009. On the prediction of extreme ecological events. *Ecol. Monogr.* **79:** 397–421.

Edwards, A. M., M. P. Freeman, G. A. Breed, and I. D. Jonsen. 2012. Incorrect likelihood methods were used to infer scaling laws of marine predator search behaviour. *PloS One* **7:** e45174.

Evangelista, D. 2014. Asterina identification and tracking routines in Python and R [Online]. Available: https://bitbucket.org/devangel77b/aquilonastra [2016, May 18].

Evangelista, D., S. Cam, T. Huynh, I. Krivitskiy, and R. Dudley. 2014. Ontogeny of aerial righting and wing flapping in juvenile birds. *Biol. Lett.* **10:** 20140497.

Ghaemi, M., Z. Zabihinpour, and Y. Asgari. 2009. Computer simulation study of the Lévy flight process. *Physica A* **388:** 1509–1514.

Humphries, N. E., N. Queiroz, J. R. M. Dyer, N. G. Pade, M. K. Musyl, K. M. Schaefer, D. W. Fuller, J. M. Brunnschweiler, T. K. Doyle, J. D. R. Houghton *et al.* 2010. Environmental context explains Lévy and Brownian movement patterns of marine predators. *Nature* **465:** 1066–1069.

Humphries, N. E., H. Weimerskirch, N. Queiroz, E. J. Southall, and D. W. Sims. 2012. Foraging success of biological Lévy flights recorded *in situ*. *Proc. Natl. Acad. Sci. USA* **109:** 7169–7174.

Jansen, V. A. A., A. Mashanova, and S. Petrovskii. 2012. Comment on "Lévy walks evolve through interaction between movement and environmental complexity." *Science* **335:** 918.

Johnson, D. S., J. M. London, M.-A. Lea, and J. W. Durban. 2008. Continuous-time correlated random walk model for animal telemetry data. *Ecology* **89:** 1208–1215.

Jones, E., T. Oliphant, and P. Peterson. 2015. SciPy: Open source scientific tools for Python, 2001 [Online]. Available: http://www.scipy.org **73:** 86 [2015, October 25].

Kareiva, P. M., and N. Shigesada. 1983. Analyzing insect movement as a correlated random walk. *Oecologia* **56:** 234–238.

Majumdar, S. N. 2010. Universal first-passage properties of discrete-time random walks and Lévy flights on a line: statistics of the global maximum and records. *Physica A* **389:** 4299–4316.

Menden-Deuer, S., and D. Grünbaum. 2006. Individual foraging behaviors and population distributions of a planktonic predator aggregating to phytoplankton thin layers. *Limnol. Oceanogr.* **51:** 109–116.

Mörters, P., and Peres, Y. 2010. *Brownian Motion*. Cambridge University Press, Cambridge.

Newman, M. E. J. 2005. Power laws, Pareto distributions and Zipf's law. *Contemp. Phys.* **46:** 323–351.

O'Loughlin, P. M., and G. Bribiesca-Contreras. 2015. New asterinid seastars from northwest Australia, with a revised key to *Aquilonastra* species (Echinodermata: Asteroidea). *Mem. Mus. Vic.* **73:** 27–40.

O'Loughlin, P. M., and J. M. Waters. 2004. A molecular and morphological revision of genera of Asterinidae (Echinodermata: Asteroidea). *Mem. Mus. Vic.* **61:** 1–40.

Olsen, T. B., F. E. G. Christensen, K. Lundgreen, P. H. Dunn, and D. A. Levitis. 2015. Coelomic transport and clearance of durable foreign bodies by starfish (*Asterias rubens*). *Biol. Bull.* **228:** 156–162.

Petrovskii, S., A. Mashanova, and V. A. A. Jansen. 2011. Variation in individual walking behavior creates the impression of a Lévy flight. *Proc. Natl. Acad. Sci. USA* **108:** 8704–8707.

Petrovskii, S., D. Bearup, D. A. Ahmed, and R. Blackshaw. 2012. Estimating insect population density from trap counts. *Ecol. Complex.* **10:** 69–82.

Pyke, G. H. 2015. Understanding movements of organisms: it's time to abandon the Lévy foraging hypothesis. *Methods Ecol. Evol.* **6:** 1–16.

Python Core Team. 2015. *Python: a Dynamic, Open Source Programming Language* [Online]. Python Software Foundation, Wilmington, DE. Available: https://ww.python.org/ [2015, Nov. 1].

R Core Team. 2015. *R: A Language and Environment for Statistical Computing* [Online]. R Foundation for Statistical Computing, Vienna, Austria. Available: http://www.R-project.org [2015, Nov. 5].

Raichlen, D. A., B. M. Wood, A. D. Gordon, A. Z. P. Mabulla, F. W. Marlowe, and H. Pontzer. 2014. Evidence of Lévy walk foraging patterns in human hunter-gatherers. *Proc. Natl. Acad. Sci. USA* **111:** 728–733.

Ramos-Fernández, G., J. L. Mateos, O. Miramontes, G. Cocho, H. Larralde, and B. Ayala-Orozco. 2004. Lévy walk patterns in the foraging movements of spider monkeys (*Ateles geoffroyi*). *Behav. Ecol. Sociobiol.* **55:** 223–230.

Reynolds, A. M., A. D. Smith, R. Menzel, U. Greggers, D. R. Reynolds, and J. R. Riley. 2007. Displaced honeybees perform optimal scale-free search flights. *Ecology* **88:** 1955–1961.

Scheibling, R. E. 1981. Optimal foraging movements of *Oreaster reticulatus* (L.) (Echinodermata: Asteroidea). *J. Exp. Mar. Biol. Ecol.* **51:** 173–185.

Sendova-Franks, A. B., and J. Van Lent. 2002. Random walk models of worker sorting in ant colonies. *J. Theor. Biol.* **217:** 255–274.

Shelton, R. M., B. E. Jackson, and T. L. Hedrick. 2014. The mechanics and behavior of cliff swallows during tandem flights. *J. Exp. Biol.* **217:** 2717–2725.

Sholtis, K. M., R. M. Shelton, and T. L. Hedrick. 2015. Field flight dynamics of hummingbirds during territory encroachment and defense. *PLoS One* **10:** e0125659.

Sims, D. W., E. J. Southall, N. E. Humphries, G. C. Hays, C. J. A. Bradshaw, J. W. Pitchford, A. James, M. Z. Ahmed, A. S. Brierley, M. A. Hindell *et al.* 2008. Scaling laws of marine predator search behaviour. *Nature* **451:** 1098–1102.

van der Walt, S., S. C. Colbert, and G. Varoquaux. 2011. The NumPy array: a structure for efficient numerical computation. *Comput. Sci. Eng.* **13:** 22–30.

Viola, P., and M. Jones. 2001. Rapid object detection using a boosted cascade of simple features. *Comput. Vis. Pattern. Recognit. Workshops* **1:** I511–I518.

Viswanathan, G. M., S. V. Buldyrev, S. Havlin, M. G. E. da Luz, E. P. Raposo, and H. E. Stanley. 1999. Optimizing the success of random searches. *Nature* **401:** 911–914.